

iMAIL

## LETTER TO THE EDITOR

### Molecular Imaging of Cardiac Allograft Rejection



Targeting Apoptosis With Radiolabeled Duramycin

About 5,400 heart transplantations are performed around the world annually. Survival in allograft recipients has improved substantially over the years with effective immunosuppressive therapy. However, acute cellular or antibody-mediated allograft rejection in the first 6 to 12 months remains a significant concern and requires close surveillance (1). Repeated endomyocardial biopsies (EMBs) are performed to detect allograft rejection. EMB is an invasive process and is associated with a finite procedural risk. Gene expression profiling in blood monocytes has been proposed as an alternative for monitoring transplant rejection with high sensitivity but has poor positive predictive value (1). Therefore, a noninvasive imaging modality would be of clinical value to define the pretest probability of acute rejection and need for EMB.

Both cell death and inflammatory cells have been targeted for noninvasive molecular imaging of graft rejection. The cell death process has been detected in vivo by imaging of cellular apoptosis, necrosis, and necroptosis (2,3). Imaging of apoptosis has targeted the exteriorization of inner cell membrane phospholipids, such as phosphatidylserine with  $^{99m}\text{Tc}$ -labeled annexin-V (4). Annexin-V is associated with significant nontarget organ radiation burden, which reduces its value for serial imaging.

Yet another phospholipid, phosphatidylethanolamine, demonstrates even greater exposure during apoptosis than phosphatidylserine. Therefore, we used the phosphatidylethanolamine-targeting radiotracer  $^{99m}\text{Tc}$ -duramycin in a heterotopic heart transplantation mouse model to mimic the immunologic response associated with varying degrees of allograft rejection, both treated and untreated (4). We hypothesized that because apoptosis increases in proportion to the severity of rejection,  $^{99m}\text{Tc}$ -duramycin could potentially assess rejection severity.

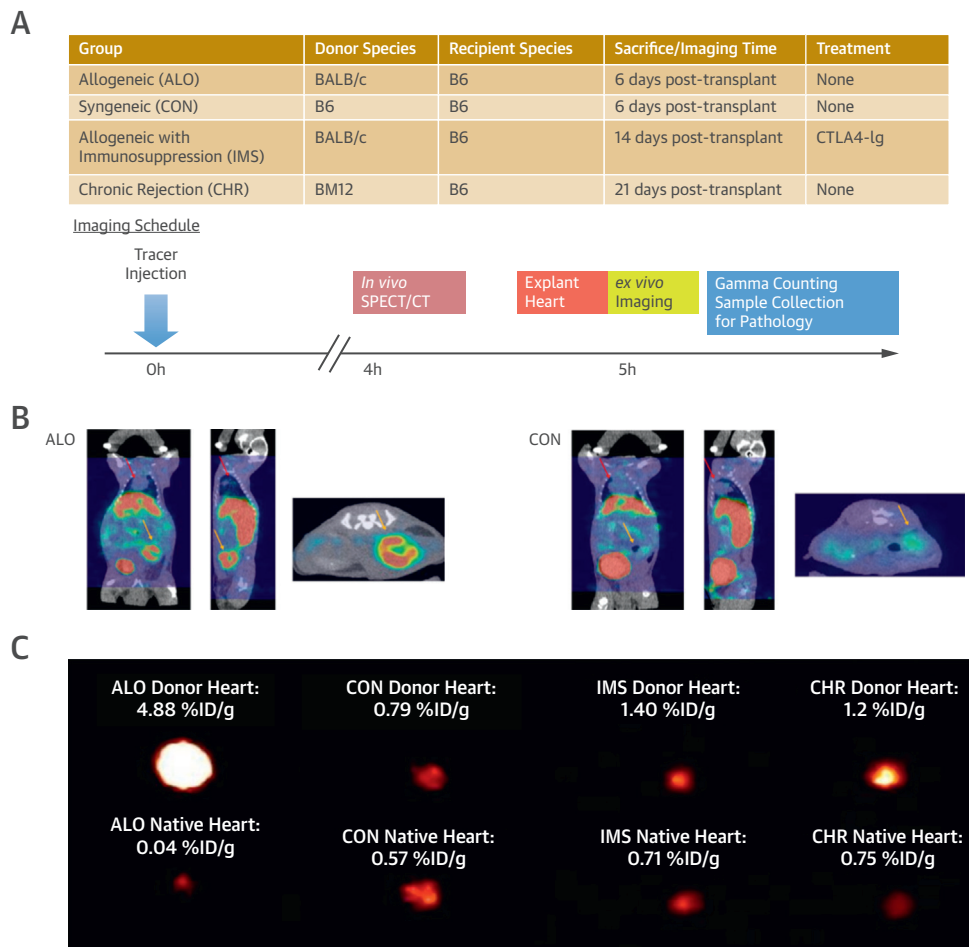
Covalently modified duramycin (Molecular Targeting Technologies, West Chester, Pennsylvania) was radiolabeled with  $^{99m}\text{Tc}$ -pertechnetate (5). In 4 groups, 19 mice received abdominal heterotopic cardiac allografts (Figure 1A). In group 1, to mimic acute

rejection, BALB/c-H2d mice hearts were transplanted into genetically different B6-H2b mice (allogeneic [ALO],  $n = 6$ ). In group 2, to demonstrate no rejection, B6 mice hearts were transplanted into genetically identical B6 mice (syngeneic control [CON];  $n = 5$ ). In group 3, to mimic acute rejection with immunosuppression treatment, BALB/c hearts were transplanted into B6 mice with CTLA4-IG immunosuppression (IMS;  $n = 4$ ). In group 4, to mimic chronic rejection (CHR), Bm12-H2bm12 mice hearts were transplanted into genetically similar, but not identical, major histocompatibility complex class II B6 mice (CHR;  $n = 4$ ).

For heterotopic heart transplantation, the donor aorta and pulmonary artery were anastomosed to the recipient aorta and vena cava, respectively. In vivo micro-single-photon emission computed tomographic/micro-computed tomographic imaging (X-SPECT, Trifoil Imaging, Chatsworth, California) of the animals was performed 4 h after  $^{99m}\text{Tc}$ -duramycin (0.6 to 0.7 mCi) administration. Fused scintigraphic-anatomic scans were evaluated in axial, sagittal, and coronal views (Figure 1B; in vivo fusion, Videos 1, 2 and 3). ALO and CON mice were imaged 6 to 7 days, IMS mice 14 to 15 days, and CHR mice 21 days following transplantation.

After in vivo imaging, transplanted and native hearts were removed and imaged ex vivo (Figure 1C). Ex vivo micro-single-photon emission computed tomographic imaging demonstrated visually significantly higher uptake in the heterotopic transplant in ALO mice, and there was relatively little to no uptake in CON and IMS mice; heterotopic hearts in CHR mice had less uptake compared with ALO mice and more compared with CON mice. Mean radiotracer uptake quantified in the region of interest (ROI) was represented as counts per square millimeter.

Hearts were then cut into 4 short-axis slices and sectioned radially into 29 to 31 pieces for gamma counting to calculate percentage injected dose per gram (%ID/g). The Kruskal-Wallis test and post hoc comparisons using Dunn's procedure were performed (R version 3.5, R Foundation for Statistical Computing) to compare differences among groups in radiotracer uptake calculated by differences in mean ROI and %ID/g between the transplanted hearts and the native hearts of each animal. Spearman's rank test was performed to correlate rejection severity with log of mean ROI counts. The mean ROI was found to be significantly different among groups ( $p < 0.01$ ) and was significantly higher in ALO compared with CON

**FIGURE 1** Molecular Imaging for Experimental Cardiac Allograft Rejection

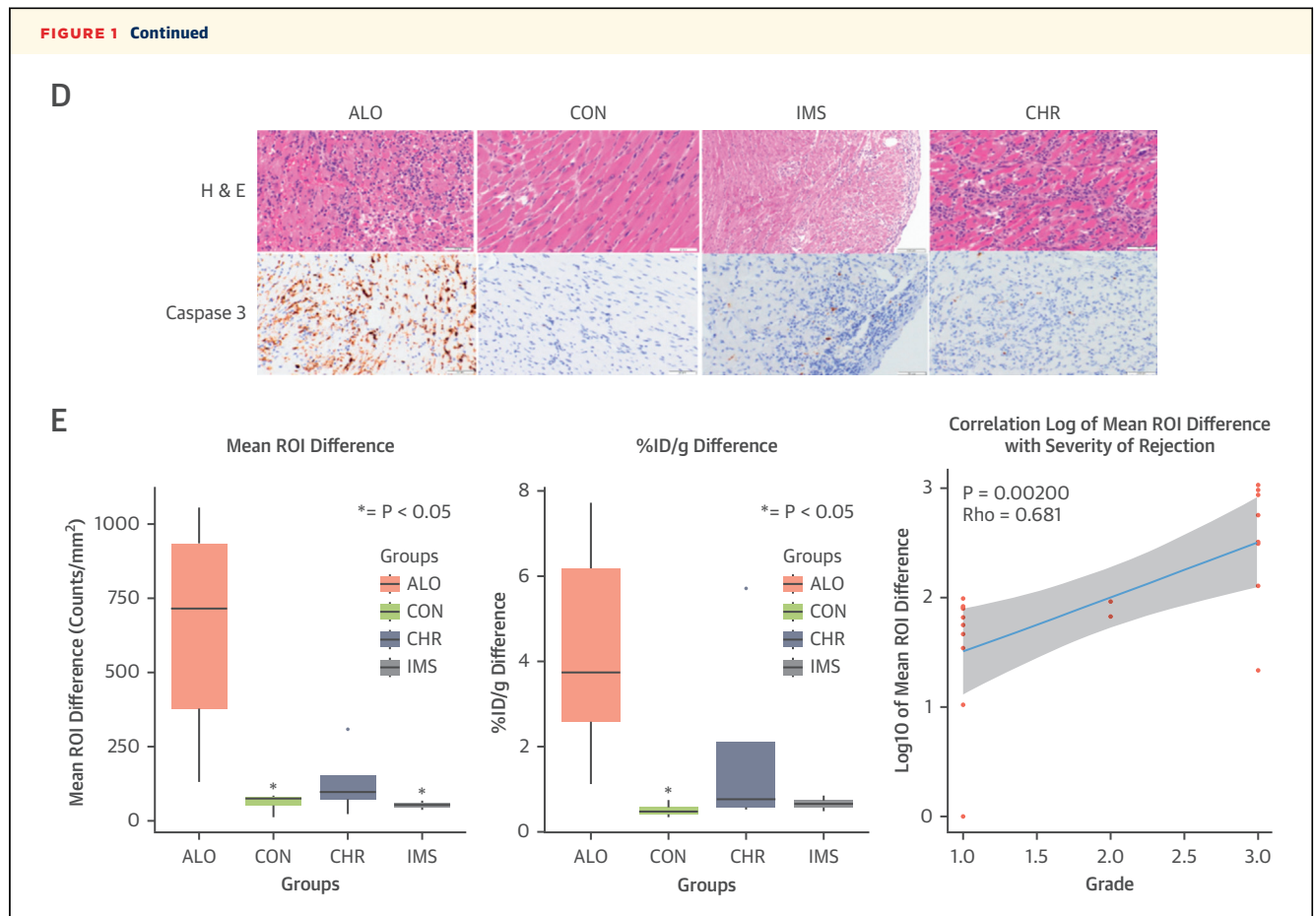
(A) Table showing the animal groups and timeline for imaging schedule. (B) In vivo micro-single-photon emission computed tomographic/micro-computed tomographic fusion images of mouse heterotopic transplantation in allogeneic (ALO) and syngeneic control (CON) groups; **yellow arrows** show heterotopically transplanted heart, and **red arrows** show native heart. (C) Ex vivo images of explanted hearts from all 4 groups with their respective percentage injected dose per gram (%ID/g) uptake values. (D) Histological characterization by hematoxylin and eosin (**top**) and caspase-3 (**bottom**) staining reveals ALO heterotopic heart with grade 3 rejection, showing interstitial hemorrhage, diffuse inflammation, and significant caspase-3 staining under high power. CON heterotopic heart with no rejection and low caspase staining. CTLA4-Ig immunosuppression (IMS) group with 1 at low power with low caspase staining. Chronic rejection (CHR) heterotopic heart with grade and low caspase-3 staining. (E) Mean region of interest (ROI) difference for each group (**left**), %ID/g difference for each group (**middle**), and scatterplot (**right**), with line of best fit showing a correlation between  $\log(\text{difference of mean ROI})$  and rejection grade severity (Videos 1, 2 and 3). ISHLT = International Society for Heart & Lung Transplantation.

Continued on the next page

and IMS mice ( $p < 0.05$ ). Similarly, %ID/g uptake was also significantly different among groups ( $p < 0.05$ ), with significantly higher uptake in ALO compared with CON mice ( $p < 0.05$ ) (Figure 1E).

Myocardial specimens underwent hematoxylin and eosin staining and apoptosis-specific caspase-3 staining. Interpretation was blindly performed by 2 pathologists (N.N. and A.L.M.). The ISHLT criteria are meant primarily for EMB, and it is difficult to obtain EMB samples in small animals. Therefore, experimental allograft rejection, in which the entire

myocardium is available for analysis, were not interpreted as EMB in ISHLT criteria. Rejection histopathology was graded according to the extent of allograft injury into grades 1 through 3, with 1 being no rejection and 3 being severe rejection; some epicardial inflammation was seen in grade 1 rejection (Figure 1D). ALO heterotopic hearts demonstrated grade 3 rejection with diffuse myocyte injury with inflammatory cell infiltrates with endothelialitis, hemorrhage, coagulative necrosis, and activated intravascular mononuclear cells. CON mice showed



no evidence of rejection of isografts. IMS animals showed epicardial inflammatory cell infiltrates with no or focal myocyte damage and minimal endothelialitis, but no hemorrhage (grade 1). CHR mice demonstrated variable degrees of myocyte damage with inflammation and variable presence of endothelialitis, mild hemorrhage, and chronic allograft vasculopathy, grades 2 to 3. Caspase-3 staining showed significant apoptosis in ALO mice but minimal staining in the CON, CHR, and IMS animals. There was a strong correlation between rejection grade and the log of mean ROI counts ( $\rho = 0.754$ ;  $p = 0.003$ ) via Spearman's rank-order correlation (Figure 1E).

This study showed the feasibility of  $^{99m}\text{Tc}$ -duramycin to noninvasively image apoptosis in correlation with cardiac allograft rejection. Despite good correlation of  $^{99m}\text{Tc}$ -duramycin with this rejection model, further studies need to determine whether these findings could be clinically translated to delineate rejection severity in allograft recipients.

Farhan Chaudhry, MS  
Matthew K.M.Y. Adapoe, BS

Kipp W. Johnson, BS  
Navneet Narula, MD  
Aditya Shekhar, BS  
Hideki Kawai, MD, PhD  
Julian K. Horwitz, MD  
Jinhua Liu, MD, PhD  
Yansui Li, MD  
Koon Y. Pak, PhD  
Jeffrey Mattis, PhD  
Andre L. Moreira, MD  
Phillip D. Levy, MD  
H. William Strauss, MD  
Artiom Petrov, PhD  
Peter S. Heeger, MD  
Jagat Narula, MD, PhD\*


\*Mount Sinai Heart  
1190 Fifth Avenue  
New York, New York 10029  
E-mail: [narula@mountsinai.org](mailto:narula@mountsinai.org)  
<https://doi.org/10.1016/j.jcmg.2020.01.010>

Please note: Drs. Pak (CEO) and Mattis (director, clinical studies) are employees of Molecular Targeting Technologies. Dr. Pak owns the patent rights to  $^{99m}\text{Tc}$ -duramycin. All other authors have reported that they have no relationships relevant to the contents of this paper to disclose.

**REFERENCES**

1. Khush K, Zarafshar S. Molecular diagnostic testing in cardiac transplantation. *Curr Cardiol Rep* 2017;19:118.
2. Ballester M, Bordes R, Tazelaar HD, et al. Evaluation of biopsy classification for rejection: relation to detection of myocardial damage by monoclonal antimyosin antibody imaging. *J Am Coll Cardiol* 1998;31:1357-61.
3. Narula J, Acio ER, Narula N, et al. Annexin-V imaging for noninvasive detection of cardiac allograft rejection. *Nat Med* 2001;7:1347-52.
4. Kalache S, Lakhani P, Heeger PS. Effects of preexisting autoimmunity on heart graft prolongation after donor-specific transfusion and anti-CD154. *Transplant J* 2014;97:12-9.
5. Kawai H, Chaudhry F, Shekhar A, et al. Molecular imaging of apoptosis in ischemia reperfusion injury with radiolabeled duramycin targeting phosphatidylethanolamine. *J Am Coll Cardiol Img* 2018;11:1823-33.

---

 **APPENDIX** For supplemental videos, please see the online version of this paper.